Heliyon 10 (2024) e22817

Contents lists available at ScienceDirect

Heliyon

journal homepage: www.cell.com/heliyon

An applicability study of rapid artificial intelligence-assisted compressed sensing (ACS) in anal fistula magnetic resonance imaging

Hao Tang [a,1], Chengdong Peng [a,1], Yanjie Zhao [a], Chenglin Hu [a], Yongming Dai [b], Chen Lin [b], Lingli Cai [a], Qiuxia Wang [a,**], Shaofang Wang [a,*]

[a] Department of Radiology, Tongji Hospital, Tongji Medical College, Huazhong University of Science and Technology, No. 1095, Jie Fang Road, Han Kou District, Wu Han, 430030, Hu Bei Province, China

[b] Shanghai United Imaging Healthcare Co., Ltd., Shanghai, 201800, China

A R T I C L E I N F O

Keywords:
Anal fistula
Magnetic resonance imaging
T2-weighted imaging
Artificial intelligence-assisted compressed sensing

A B S T R A C T

Objective: To evaluate the applicability of artificial intelligence-assisted compressed sensing (ACS) to anal fistula magnetic resonance imaging (MRI).

Methods: 51 patients were included in this study and underwent T2-weighted sequence of MRI examinations both with ACS and without ACS technology in a 3.0 T MR scanner. Subjective image quality scores, and objective image quality-related metrics including scanning time, signal-to-noise ratio (SNR), and contrast-to-noise ratio (CNR), were evaluated and statistically compared between the images collected with and without ACS.

Results: No significant difference in the subjective image quality of lesion conspicuity was observed between the two groups. However, ACS MRI decreased the acquisition time with regard to control group (74.00 s vs. 156.00 s). Besides, SNR of perianal and muscle in the ACS group was significantly higher than that of the control group (164.07 ± 33.35 vs 130.81 ± 29.10, $p < 0.001$; 109.87 ± 22.01 vs 87.61 ± 17.95, $p < 0.001$; respectively). The CNR was significantly higher in the ACS group than in the control group (54.02 ± 23.98 vs 43.20 ± 21.00; $p < 0.001$). Moreover, the accuracy rate of the ACS groups in evaluating the direction and internal opening of the fistula was 88.89 %, exactly the same as that of the control group.

Conclusion: We demonstrated the applicability of using ACS to accelerate MR of anal fistulas with improved SNR and CNR. Meanwhile, the accuracy rates of the ACS group and the control were equivalent in evaluating the direction and internal opening of the fistula, based on the results of surgical exploration.

Abbreviations: ACS, artificial intelligence-assisted compressed sensing; MRI, magnetic resonance imaging; SNR, signal-to-noise ratio; CNR, contrast-to-noise ratio; DRE, digital rectal examination; HF, half Fourier; PI, parallel imaging; CS, compressed sensing; T2WI, T2-weighted imaging sequences; FSE, fast spin echo; TR, repetition time; TE, echo time; FOV, field of view; NEX, number of excitations; PACS, picture archiving and communication system; SD, standard deviation.

* Corresponding author.
** Corresponding author.
E-mail addresses: wangqiuxia@hust.edu.cn (Q. Wang), wangshaofang2020@outlook.com (S. Wang).

[1] Hao Tang and Chengdong Peng contributed equally.

https://doi.org/10.1016/j.heliyon.2023.e22817
Received 21 December 2022; Received in revised form 15 November 2023; Accepted 20 November 2023
Available online 6 December 2023

Anal fistula is an inflammatory condition defined by an abnormal granulomatous connection between the anal canal and the skin of the perineum, mainly involving the anal canal [1]. Effective treatments that reduce recurrence rates and avoid side effects depend on accurate detection and characterization of the anal fistula. Optimal treatment requires detailed preoperative imaging information, including the location of the fistula and affected pelvic structure. Assessment of fistula characteristics, such as fistula classification, detection, and direction of the internal opening, as well as any secondary site that may extend or form an abscess, are essential for accurate management [2,3].

Various techniques, including digital rectal examination (DRE), intraluminal sonography, contrast radiography, X-ray computed tomography, and MRI, can be used for the preoperative assessment of anal fistulas [4–6]. However, each technique has certain disadvantages. For example, DRE shows a low diagnostic accuracy, and CT has a low soft tissue resolution and is thus unable to distinguish minute fistulas from abscesses in time [7]. MR has emerged as another popular imaging technique of choice for the preoperative evaluation of perianal fistulas because of its multi-planar imaging and high soft tissue contrast, providing a highly accurate, rapid, and noninvasive means for pre-surgical assessment [8]. However, the long scan times associated with most clinically relevant sequences that contribute to increased costs and limited the use of MRI may not only reduce the comfort and cooperation of very young or old patients with poor tolerance, but also add burden to the arrangement of the heavy clinical tasks in the radiology department.

To overcome this limitation, many effective methods have been introduced for imaging acceleration, such as half-Fourier (HF) [9], parallel imaging (PI) [10], and compressed sensing (CS) [11]. However, each of these single-acceleration techniques has several disadvantages. For example, routinely used PI could decrease the image quality at high acceleration by noise amplification and/or undersampling artifacts [12]. Moreover, insufficient sparseness may lead to noise-like aliasing artifacts when an excessively high acceleration factor is employed in the CS [11,13]. Theoretically, the disadvantages of a single method can be avoided by combining multiple techniques. A previous study showed that several combinations of accelerations provided significantly better image quality, lesion conspicuity, and lesion detectability compared with conventional abdominal MRI sequence [14]. The AI technique that realizes deep learning-based data collection and reconstruction can effectively correct significant errors in these individual techniques in time [15]. Based on the above theories and practical study, artificial intelligence-assisted compressed sensing (ACS) MR imaging, which combines the AI module with HF, PI, and CS for noise suppression, information recovery, and artifact reduction, has been developed as a novel MR acceleration solution to achieve the best balance speed and image quality in kidney MR imaging [16]. However, the application of ACS in anal fistula imaging has not been reported. Therefore, the objective of this study was to explore a new rapid ACS sequence for anal fistulas imaging by comparing the subjective and objective image quality and evaluating the possibility of its future routine application.

1. Materials and methods

1.1. Patients

This prospective study was performed on patients who underwent anal fistula MR in our hospital between January 2021 and September 2021. T2-weighted imaging (T2WI) sequences, including both ACS (ACS group) and without ACS (control group), were performed. The exclusion criteria were as follows: (1) patients with contraindications to MRI examination and (2) patients with poor-quality images obtained during the scanning procedures. Both sequences maintained the same imaging position and thickness in the same patient. This study was approved by the ClinicalTrials.gov (ID: NCT02337777), the Institutional Review Board of Tongji Hospital of Tongji Medical College (ID:TJ-IRB20211123), HUST, and the requirement for formal informed consent was obtained from all patients.

1.2. MR image acquisition

Patients underwent MRI examinations with a 3.0T MR scanner (uMR 790, United Imaging Healthcare Co., Ltd. (UIH), Shanghai, China) with a 12-channel torso coil (phased-array body coil) and a column matrix body coil in the supine position. Common MRI techniques for anal fistulas include standardized sagittal fat-suppressed T2-weighted fast spin-echo (FSE) and axial T1-weighted FSE sequences, high-resolution axial T2WI, and coronal fat-suppressed T2WI sequences. Therefore, a sequence in the sagittal plane with a 45-degree slope forward from the vertical direction was performed first. The axial (i.e., the conventional position for the diagnosis or treatment of anal diseases, which corresponds to the surgeon's point of view and facilitates the location of the leak) and coronal sequences must be aligned with the anal canal in the sagittal sequence, oriented perpendicular and parallel to the long axis of the anal canal, respectively. ACS technology [14] in this study has been FDA-approved for accelerating image acquisition using an extended fully convolutional neural networks (CNN). HF and PI are all incorporated into the AI model for noise suppression, information recovery, and artifact reduction.

1.3. Imaging analysis

1.3.1. Diagnostic evaluations

In this study, to compare the diagnostic effectiveness of anal fistulas with surgical results, careful evaluation of the following data was performed on a dedicated workstation by senior radiologists: direction of fistula (whether simple or branching), internal opening, and distance between the internal opening and anal verge (location). The direction of the fistula was identified on axial images using the "anal clock'' [2]. Moreover, the categories of anal fistula were evaluated according to Parks' classification (Grade1, intersphincteric fistula; grade 2, transsphincteric fistula; grade 3, suprasphincteric fistula; and grade 4, extrasphincteric fistula) [3].

1.3.2. Subjective assessment of image quality

Image quality was subjectively assessed by two different experienced radiologists. The scoring criteria were as follows [17]: displayed anatomical details (1 = poor, 2 = fair, 3 = good, 4 = excellent); distortion (1 = severe, 2 = moderate, 3 = slight, 4 = absent); artifacts (1 = serious, 2 = moderate, 3 = slight, 4 = absent); lesion conspicuity (1 = poor, considered unrecognized; 2 = fair, most of the outlines unclear; 3 = good, small part of the outline unclear; 4 = excellent, clear outline).

1.3.3. Objective assessment of image quality

All MR images were observed and analyzed on a picture archiving and communication system (PACS) and a UIH workstation in our hospital. Radiologists with more than five years of experience co-evaluated the ACS and control group images. Three layers with good image quality were selected, and regions of interest (ROI) of the same size at three positions in the perianal, background, and muscle tissues were gauged and calculated. Standard deviation (SD) was used as the image noise.

The average values of the measured data were calculated to minimize errors. The signal-to-noise ratio (SNR) and contrast-to-noise ratio (CNR) were calculated as follows:

$$\mathrm{SNR}\ \overline{x}_{\mathrm{perianal}} = \mathrm{SI}\ \overline{x}_{\mathrm{perianal}} \Big/ \ \mathrm{SD}\ \overline{x}_{\mathrm{background}}$$

$$\mathrm{SNR}\ \overline{x}_{\mathrm{muscle}} = \mathrm{SI}\ \overline{x}_{\mathrm{muscle}} \Big/ \ \mathrm{SD}\ \overline{x}_{\mathrm{background}}$$

$$\mathrm{CNR} = \left| \mathrm{SI}\ \overline{x}_{\mathrm{perianal}} \text{-} \mathrm{SI}\overline{x}_{\mathrm{muscle}} \right| / \ \mathrm{SD}\ \mathrm{SD}\ \overline{x}_{\mathrm{background}}$$

Note: SI $^{-}\mathrm{X}_{\mathrm{perianal}}$ is the mean signal intensity of perianal, SD$^{-}\mathrm{X}_{\mathrm{background}}$ is the standard deviation of background noise, and SI $^{-}\mathrm{X}_{\mathrm{muscle}}$ is the mean signal intensity of the muscle.

1.4. Statistical analysis

Statistical analyses were performed using SPSS version 26 (IBM, Armonk, NY, USA) and GraphPad Prism. Statistical values, including SCR and CNR, are presented as mean ± standard deviation. A paired independent samples *t*-test was applied to compare the differences in the locations, SNRs, and CNRs between the ACS and control groups. The interrater reliability of the two radiologists was assessed by both weighted Kappa Coefficient [18] (Kappa value, $\kappa > 0.8$, excellent agreement; $0.60 \le \kappa \le 0.80$, good agreement; $0.40 \le \kappa < 0.60$, moderate agreement; $0.20 \le \kappa < 0.40$, fair agreement; $\kappa < 0.20$, poor agreement) and Intraclass Correlation Coefficient [19] (ICCs, ICC > 0.90, excellent agreement; 0.75≤ ICC < 0.9, good agreement; 0.5≤ ICC < 0.75, moderate agreement; ICC < 0.5, poor agreement). To determine the agreement of correct diagnostic effectiveness between ACS/control MRI and surgical results, the kappa statistic was used and the 95 % confidence intervals (CIs) was obtained. Wilcoxon test was used for the comparison the direction (o'clock), internal opening and category between ACS and control group. A P value of less than 0.05 was considered to indicate a statistically significant difference.

2. Results

2.1. Clinical characteristics

Between January 2021 and December 2021, 51 patients (41 males and 10 females with; age range, 16–71 years; average age, 33.2 years were enrolled in this study. Both subjective and objective assessments of the image quality were evaluated. Table 1 shows the patient characteristics in this study.

Table 1
The patients' characteristics in this study.

Characteristics	Number of Patients (%)
Sex	
Male	41 (80.39)
Female	10 (19.61)
Year	
≤20	13 (25.49)
(20, 30]	13 (25.49)
(30, 40]	13 (25.49)
(40, 50]	5 (9.80)
(50, 60]	4 (7.84)
> 60	3 (5.88)
Treatment	
No surgical	33 (64.71)
Surgical	18 (35.29)

2.2. Comparison of acquisition time in a series of typical ACS and control sequences

The acquisition times of different sequences in the ACS and control groups were compared. As shown in Table 2, the ACS group allowed faster scanning with a nearly 2-fold accelerated scan time in each sequence for the same three-plane scanning. Detailed parameters of the important Axi-T2WI sequence are compared in Table 2.

2.3. Results of diagnostic evaluation

Diagnostic categories were collected from patients treated surgically in the ACS and control groups (Table 3). The details of each category assessed in the patients are presented in supplement Table 1 (S. Table 1). In addition, we assessed the direction of the fistula, internal opening, and location (distance between the internal opening and anal verge, cm) between the two imaging groups. Based on the results of the surgical exploration, the accuracy rates of the ACS and control groups in evaluating the direction and internal opening of the fistula were 88.89 % and 88.89 %, respectively. No significant differences were observed between these assessments. The location (cm) was 2.372 ± 0.985 vs. 2.261 ± 0.989 between the ACS and control groups, with no significant difference ($p > 0.05$). (Fig. 1).

3. Results of subjective assessment

Two radiologists subjectively used the same evaluation criteria to score the anatomical details, artifacts, and lesion conspicuity of the ACS and control groups. Although there were no significant differences in these subjective image scores (Fig. 2), we noted that several ACS images (Fig. 3A and C) had better quality than those of the control groups (Fig. 3B and D). The image anatomical details (Fig. 2A), artifacts (Fig. 2B), and lesion conspicuity scores (Fig. 2C) were: 3.922 ± 0.271 vs. 3.824 ± 0.385, $p = 0.133$; 3.882 ± 0.325 vs 3.902 ± 0.300 $p = 0.743$; 3.902 ± 0.300 vs 3.863 ± 0.348 $p = 0.532$.

The inter- and intra-observer reliabilities of the two radiologists were assessed using both weighted kappa and intraclass correlation coefficients. All subjective scores were in good inter-observer agreement with the details shown in Table 4.

3.1. Results of objective assessment

The perianal SNR of the ACS group was significantly higher than that of the control group (166.8 ± 6.116 vs 134.1 ± 5.165; $p < 0.001$) (Fig. 4A). Likewise, the muscle SNR of the ACS group was also significantly higher than that of the control group (110.1 ± 3.584 vs 89.04 ± 2.607; $p < 0.001$) (Fig. 4B). Moreover, the CNR of the ACS group was significantly higher than that of the control group (56.74 ± 4.448 vs 45.10 ± 3.940; $p < 0.001$) (Fig. 4C).

4. Discussion

In this study, based on the results of surgical exploration, the accuracy rate of the ACS groups in evaluating the direction and internal opening of the fistula was 88.89 %, exactly the same as that of the control group. Moreover, the evaluation of anal fistulas in the ACS group was better with a 2-fold accelerated scan time in comparison with the control group. In summary, ACS MRI provides a rapid scanning method for examining patients with special anal fistulas, with the benefits of higher imaging efficiency and better patient tolerance.

We demonstrated the feasibility of using ACS to accelerate MR imaging of anal fistulas, which did not decrease the subjective assessment of image quality; instead, it could increase the objective assessment, including SNR and CNR. A previous study showed that subjective and objective assessment in the clinical practice of radiology was dominated by the consideration of medical image quality [20]. Accordingly, we based our study on the blinded clinical assessment of MRI images. In addition to the subject image quality, we

Table 2
Comparison of T2WI sequence parameters between ACS and control groups.

Parameters	ACS	Control
Acquisition time (s)	74	156
TR (ms)	2820	2219
TE (ms)	72.9	71.54
FOV (mm^2)	200*200	200*200
Slice Thickness (mm)	3	3
No. of slice	30	30
NEX	2	2
Flip(°)	110	110
Voxel size(mm)	0.93 × 0.83 × 3	0.93 × 0.83 × 3
Bandwidth (kHz)	260	200
Echo length	19	11
Echo interval (ms)	8.1	10.22
Acceleration	ACS	PI

Note: TR, repetition time; TE, echo time; FOV, field of view; NEX, number of excitations.

Table 3
Comparison of the correct diagnostic effectiveness.

	ACS n (%)	Control n (%)	P
Direction			
Correct	16 (88.89)	16 (88.89)	
Incorrect	2 (11.11)	2 (11.11)	
Internal opening			
Correct	16 (88.89)	16 (88.89)	
Incorrect	2 (11.11)	2 (11.11)	
Category			> 0.05
Grade 1	10	11	
Grade 2	6	5	
Grade 3	1	1	
Grade 4	1	1	

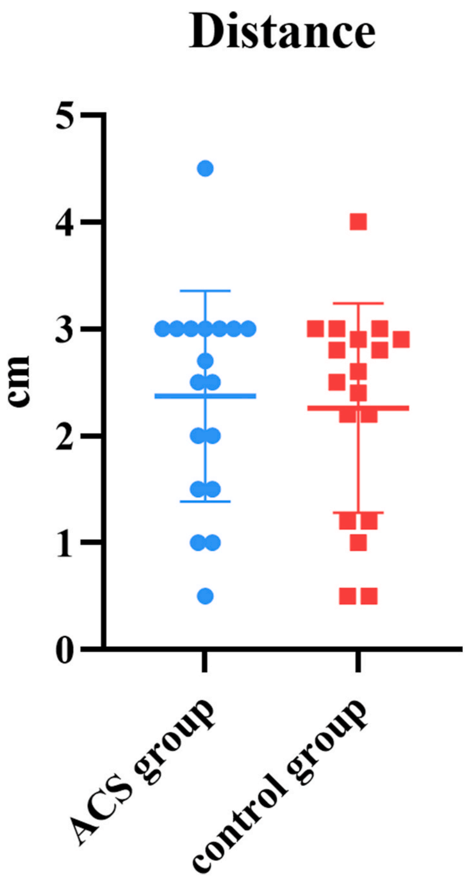

Fig. 1. Comparison of location (cm) results between ACS and control groups.

focused on SNR and CNR. SNR is one of several important quality metrics frequently used for the assessment of medical images and is often used to describe the performance of an MRI system [21,22]. Generally, a higher SNR indicates a more appealing and smoother image for the reader. Changing the scan parameters, slice thickness, and field of view can change the SNR in MR images because of their effect on background noise [21]. ACS technique allows us to achieve better SNR without compromising slice thickness, resolution, and other scan parameters. T2WI images provide sufficient information to guide surgical treatment and to identify active inflammation due to the excellent soft tissue contrast to the pelvic organs [23]. Active inflammation appears hyperintense on T2-weighted images due to the presence of large amounts of pus and granulation tissues [23]. In addition, T2WI sequences based on 2D FSE, which are performed in multiple planes, play a critical role in the basic routine protocols for patients with anal fistulas [24,25]. Therefore, this study focused on the comparative analysis of transverse images of T2WI sequences with different acceleration modes.

Our study used 3.0-T MR imaging equipment (UIH, Shanghai, China) with a high field strength, which potentially provides better and higher time resolution. Moreover, the ACS acceleration technology in this study was used for anal fistulas to evaluate the imaging speed and quality and thus analyze whether the final image provided by ACS can satisfy the clinical diagnosis and shorten the scan

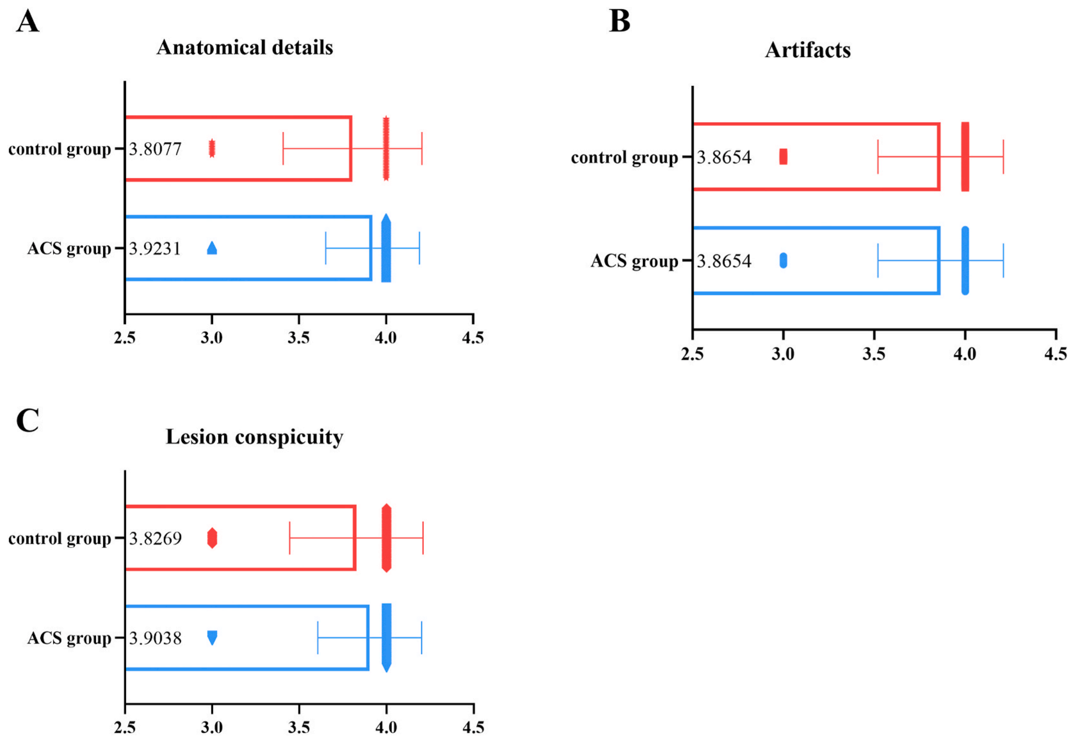

Fig. 2. Subject assessment of image quality including anatomical details(A), artifacts(B) and lesion conspicuity(C). There are no significant differences in the assessment scores in the above analyze contents.

time. Here, ACS still employs CS technology, whereas an AI module based on a deep learning neural network was innovatively introduced to accelerate the filling of k-space. ACS can effectively correct any significant errors in these methods by combining AI modules with HF, PI, and CS technologies, which can suppress noise, reduce artifacts, and compress the perception of recovered information, thus allowing a higher acceleration level for MR imaging. The final images provided by the ACS were excellent for clinical diagnosis, with increased SNR and CNR. In short, ACS of anal fistulas, providing a faster imaging speed and thus reduced motion artifacts, not only allowed us to perform more comprehensive examinations in a short amount of time but also improved patient comfort and experiences. In addition, imaging of anal fistulas needs to be developed to increase the number of 3D sequences to better assist in clinical quality diagnosis. 3D imaging, with advantages including a higher SNR and reduced imaging time, provides thinner cross-sections and covers larger volumes without operator dependence when obliquely collecting images [18]. The usefulness of 3D T2WI imaging sequences in rectal cancer and female pelvis has been evaluated [24]. Our next research goal is to achieve 3D T2WI imaging in fast ACS imaging.

Our study had certain limitations. Primarily, the sample size is relatively small, although the statistics reached significant criteria, future study with larger sample sizes are required for detailed comparisons of anal fistula of different stages. Secondly, only the SNR and CNR of the transverse images were compared at the same location in the same patient. Other images, such as sagittal T2WI and coronal T2WI, were used with ACS acceleration to acquire clinical imaging information. In case of image quality bias caused by individual differences of the scanner operators, it is necessary for the operators or technicians to keep communication with the diagnostic physicians to adjust the imaging mode and parameters in time for each individual scanning to ensure the success of clinically accurate image acquisition for each patient. Third, the 3-mm thick slices used for transverse T2WI were too thick to identify small anal fistulas. However, this slice thickness was commonly used in previous studies. A better spatial resolution of 3D T2WI imaging accelerated by fast ACS technique may overcome this limitation.

In summary, the application of ACS MR for anal fistulas provided a higher subjective image perceptions and better image qualities. Furthermore, ACS images provided higher SNR and CNR provided clear parameters for assessing the accuracy of imaging information on the location of the fistulas and the affected pelvic structure. In addition, a 50 % reduction in the acquisition time was convenient for preoperative diagnosis and postoperative evaluation, especially in uncooperative patients whose images may be affected severely by motion artifacts. Furthermore, the course of the fistula and the site of any secondary abscess can be rapidly evaluated, which can alleviate the heavy burden of clinical auxiliary medicine and make the diagnosis and treatment more efficient.

Ethics approval and consent to participate

This study was approved by the ClinicalTrials.gov (ID: NCT02337777), the Institutional Review Board of Tongji Hospital of Tongji

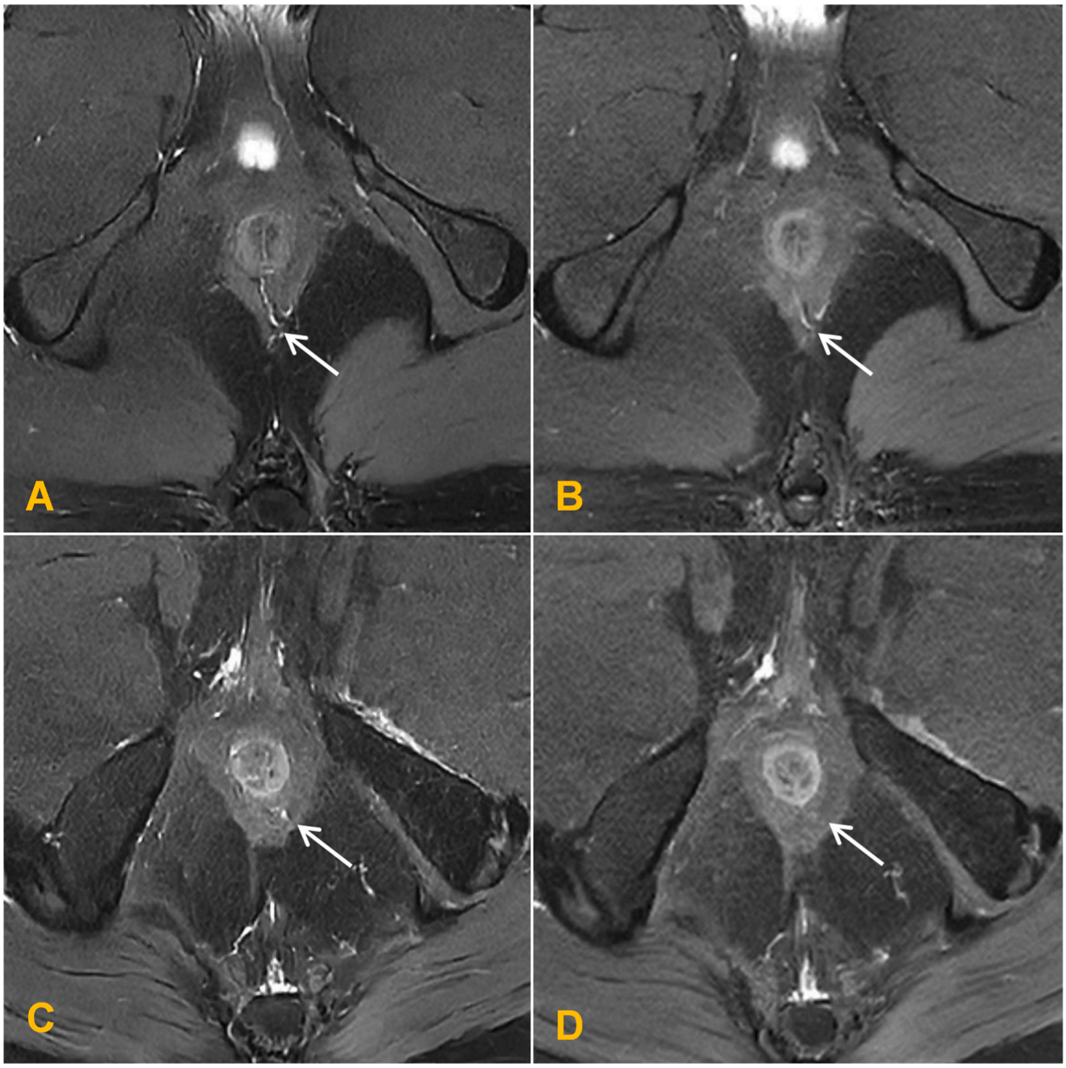

Fig. 3. Example of subjective quality between ACS (A, C) and control (B, D) Axi-T2WI images.

Table 4
Interrater reliability of subject assessment between the two radiologists.

Subject Assessment	ACS mean (SD)				Control mean (SD)			
	R1	*R2*	κ	*ICC*	*R1*	*R2*	κ	*ICC*
Anatomical details	3.922 (0.271)	3.941 (0.238)	0.847	0.849	3.824 (0.385)	3.843 (0.367)	0.929	0.964
Artifacts	3.882 (0.325)	3.902 (0.300)	0.898	0.900	3.902 (0.300)	3.922 (0.272)	0.878	0.936
Lesion conspicuity	3.902 (0.300)	3.922 (0.272)	0.878	0.880	3.863 (0.348)	3.882 (0.325)	0.912	0.955

Medical College (ID:TJ-IRB20211123), HUST, and the requirement for formal informed consent was obtained from all patients. We confirm that participants consented to have these images published.

Authors' declaration

I would like to declare on behalf of my co-authors that the work described was original research that has not been published previously, and not under consideration for publication elsewhere, in whole or in part. All the authors listed have approved the manuscript that is enclosed.

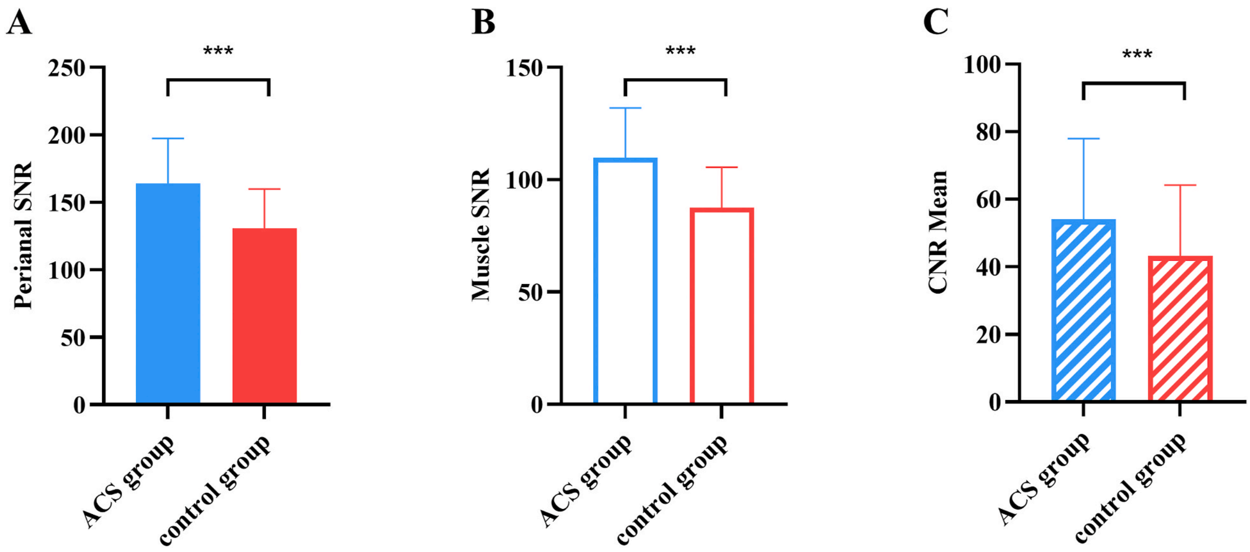

Fig. 4. Comparison of SNR and CNR of different ROI positioning protocols. The perianal and muscle SNR as well as the mean CNR of the ACS group were compared with those of the control group in histograms. (A) Mean and standard error of the mean (SEM) of the perianal SNR for the ACS and control groups. (B) Mean and SEM of the muscle SNR of the ACS and control groups. (C) Mean and SEM of the CNR of the ACS and control groups. Statistical analysis was performed using paired *t*-tests, and *** indicates statistical significance ($p < 0.001$).

Data availability statement

The data that support the findings of this study are available from the corresponding author, [Shaofang Wang], upon reasonable request.

Competing financial interests

We, the authors and our immediate family members, have no financial interests to declare.

Funding

This work was supported by the Grant from the Natural Science Foundation of Hubei Province (2022CFB205), China.

CRediT authorship contribution statement

Hao Tang: Writing – original draft, Methodology, Formal analysis, Conceptualization. **Chengdong Peng:** Writing – original draft, Investigation, Formal analysis, Conceptualization. **Yanjie Zhao:** Visualization, Validation. **Chenglin Hu:** Visualization, Software. **Yongming Dai:** Supervision, Software. **Chen Lin:** Supervision, Software. **Lingli Cai:** Visualization, Formal analysis. **Qiuxia Wang:** Writing – review & editing, Validation, Supervision, Investigation, Funding acquisition, Conceptualization. **Shaofang Wang:** Writing – review & editing, Writing – original draft, Visualization, Project administration, Methodology, Investigation, Formal analysis, Data curation, Conceptualization.

Declaration of competing interest

The authors declare that they have no known competing financial interests or personal relationships that could have appeared to influence the work reported in this paper.

Acknowledgements

We would like to express our gratitude to everyone who took part in this project. We especially thank Xiaopeng Song from Central Research Institute, United Imaging Healthcare, Shanghai, China for the technical guidance and language modification.

Appendix A. Supplementary data

Supplementary data to this article can be found online at https://doi.org/10.1016/j.heliyon.2023.e22817.

References

[1] K.S. Jhaveri, S. Thipphavong, L. Guo, M.G. Harisinghani, MR imaging of perianal fistulas, Radiol. Clin. 56 (5) (2018) 775–789, https://doi.org/10.1016/j.rcl.2018.04.005.
[2] N. Ramírez Pedraza, A.H. Pérez Segovia, J.A. Garay Mora, et al., Perianal fistula and abscess: an imaging guide for beginners, Radiographics 42 (7) (2022) E208–E209, https://doi.org/10.1148/rg.210142.
[3] X. Liu, Z. Wang, H. Ren, et al., Evaluating postoperative anal fistula prognosis by diffusion-weighted MRI, Eur. J. Radiol. 132 (2020), 109294, https://doi.org/10.1016/j.ejrad.2020.109294.
[4] L.M. Minordi, A. Bevere, A. Papa, L. Larosa, R. Manfredi, CT and MRI evaluations in crohn's complications: a guide for the radiologist, Acad. Radiol. 29 (8) (2022) 1206–1227, https://doi.org/10.1016/j.acra.2021.07.025.
[5] I. Sudoł-Szopińska, G.A. Santoro, M. Kołodziejczak, A. Wiaczek, U. Grossi, Magnetic resonance imaging template to standardize reporting of anal fistulas, Tech. Coloproctol. 25 (3) (2021) 333–337, https://doi.org/10.1007/s10151-020-02384-6.
[6] M. Biondi, E. Bicci, G. Danti, et al., The role of magnetic resonance enterography in crohn's disease: a review of recent literature, Diagnostics 12 (5) (2022) 1236, https://doi.org/10.3390/diagnostics12051236.
[7] K.B. Waheed, W.J. Shah, B. Altaf, et al., Magnetic resonance imaging findings in patients with initial manifestations of perianal fistulas, Ann. Saudi Med. 40 (1) (2020) 42–48, https://doi.org/10.5144/0256-4947.2020.42.
[8] S.P. Sheedy, D.H. Bruining, E.J. Dozois, W.A. Faubion, J.G. Fletcher, MR imaging of perianal crohn disease, Radiology 282 (3) (2017) 628–645, https://doi.org/10.1148/radiol.2016151491.
[9] J. Walheim, A. Gotschy, S. Kozerke, On the limitations of partial Fourier acquisition in phase-contrast MRI of turbulent kinetic energy, Magn. Reson. Med. 81 (1) (2019) 514–523, https://doi.org/10.1002/mrm.27397.
[10] T. Aoike, N. Fujima, M. Yoneyama, et al., Development of three-dimensional MR neurography using an optimized combination of compressed sensing and parallel imaging, Magn. Reson. Imag. 87 (2022) 32–37, https://doi.org/10.1016/j.mri.2021.12.002.
[11] A. Bustin, N. Fuin, R. Botnar, C. Prieto, From compressed-sensing to artificial intelligence-based cardiac MRI reconstruction, Front. Cardiovasc. Med. 7 (2020) 17, https://doi.org/10.3389/fcvm.2020.00017.
[12] H. Demirturk Kocasarac, E.S. Kursun-Cakmak, G. Ustaoglu, S. Bayrak, K. Orhan, M. Noujeim, Assessment of signal-to-noise ratio and contrast-to-noise ratio in 3 T magnetic resonance imaging in the presence of zirconium, titanium, and titanium-zirconium alloy implants, Oral Surg. Oral Med. Oral Pathol. Oral Radiol. 129 (1) (2020) 80–86, https://doi.org/10.1016/j.oooo.2019.08.020.
[13] R. Kijowski, H. Rosas, A. Samsonov, K. King, R. Peters, F. Liu, Knee imaging: rapid three-dimensional fast spin-echo using compressed sensing, J. Magn. Reson. Imag. 45 (6) (2017) 1712–1722, https://doi.org/10.1002/jmri.25507.
[14] R-f Sheng, L-y Zheng, K-p Jin, et al., Single-breath-hold T2WI liver MRI with deep learning-based reconstruction: a clinical feasibility study in comparison to conventional multi-breath-hold T2WI liver MRI, Magn. Reson. Imag. 81 (2021) 75–81, https://doi.org/10.1016/j.mri.2021.06.014.
[15] H. Ben Yedder, B. Cardoen, G. Hamarneh, Deep learning for biomedical image reconstruction: a survey, Artif. Intell. Rev. 54 (1) (2021) 215–251, https://doi.org/10.1007/s10462-020-09861-2.
[16] Y. Zhao, C. Peng, S. Wang, X. Liang, X. Meng, The feasibility investigation of AI -assisted compressed sensing in kidney MR imaging: an ultra-fast T2WI imaging technology, BMC Med. Imag. 22 (1) (2022) 119, https://doi.org/10.1186/s12880-022-00842-1.
[17] M. Chen, C. Feng, Q. Wang, et al., Comparison of reduced field-of-view diffusion-weighted imaging (DWI) and conventional DWI techniques in the assessment of Cervical carcinoma at 3.0T: image quality and FIGO staging, Eur. J. Radiol. 137 (2021), 109557, https://doi.org/10.1016/j.ejrad.2021.109557.
[18] J. Zhao, F. Lu, Q. Wang, et al., Comparison of contrast-enhanced fat-suppressed T1-3D-VIBE and T1-TSE MRI in evaluating anal fistula, Abdominal Radiol. 47 (11) (2022) 3688–3697, https://doi.org/10.1007/s00261-022-03661-8.
[19] T.K. Koo, M.Y. Li, A guideline of selecting and reporting intraclass correlation coefficients for reliability research, J. Chiropractic Med. 15 (2) (2016) 155–163, https://doi.org/10.1016/j.jcm.2016.02.012.
[20] N. Sinha, A.G. Ramakrishnan, Quality assessment in magnetic resonance images, Crit. Rev. Biomed. Eng. 38 (2) (2010) 127–141, https://doi.org/10.1615/critrevbiomedeng.v38.i2.20.
[21] Y. Lee, B.J. Wilm, D.O. Brunner, et al., On the signal-to-noise ratio benefit of spiral acquisition in diffusion MRI, Magn. Reson. Med. 85 (4) (2021) 1924–1937, https://doi.org/10.1002/mrm.28554.
[22] M. Oszust, M. Bielecka, A. Bielecki, I. Ste¸pień, R. Obuchowicz, A. Piórkowski, Blind image quality assessment of magnetic resonance images with statistics of local intensity extrema, Inf. Sci. 606 (2022) 112–125, https://doi.org/10.1016/j.ins.2022.05.061.
[23] J. Baik, S.H. Kim, Y. Lee, J.-H. Yoon, Comparison of T2-weighted imaging, diffusion-weighted imaging and contrast-enhanced T1-weighted MR imaging for evaluating perianal fistulas, Clin. Imag. 44 (2017) 16–21, https://doi.org/10.1016/j.clinimag.2017.03.019.
[24] S. Halligan, Magnetic resonance imaging of fistula-in-ano, Magn. Reson. Imag. Clin. N. Am. 28 (1) (2020) 141–151, https://doi.org/10.1016/j.mric.2019.09.006.
[25] S.-T. Feng, M. Huang, Z. Dong, et al., MRI T2-weighted imaging and fat-suppressed T2-weighted imaging image fusion technology improves image discriminability for the evaluation of anal fistulas, Korean J. Radiol. 20 (3) (2019) 429–437, https://doi.org/10.3348/kjr.2018.0260.